THE BELL SYSTEM TECHNICAL JOURNAL
Vol. 52, No. 3, March, 1973
Printed in U.S.A.

Slope Overload Noise in Linear Delta Modulators With Gaussian Inputs

By L. J. GREENSTEIN

(Manuscript received September 22, 1972)

This paper derives a slope overload noise power formula for linear delta modulators having ideal integrators and Gaussian random inputs. Although the same problem has been treated by others, the present result is the only one applicable to all slope-following capacities and input spectra.

Despite its singleness of purpose, the paper divides logically into two parts. In Part 1, a common element in all previously published results is used to derive a new slope overload noise power formula. This derivation is analytically rigorous and provides some useful insights, but pertains to a particular kind of spectrum and so is incomplete.

The more universal result we seek is derived in Part 2. The approach here is far less rigorous and amounts to approximating the influences of other kinds of spectra by modifying the result of Part 1. The final expression contains four spectrum-related coefficients, for which simple formulas are given, and has an estimated accuracy of 1 dB for all cases of practical interest. Computed results are given for two important families of spectra and comparisons are made with previously published results.

Part 1

I. INTRODUCTION

1.1 *Objective*

This paper presents some new theoretical results on slope overload noise in linear delta modulators. In particular, we derive the mean power of the (unfiltered) slope overload noise at the demodulator output when the modulator input is a stationary Gaussian random process and the modulator feedback path contains an ideal integrator, Fig. 1. This same problem has already been treated by other investigators, notably Zetterberg,[1] Rice (with O'Neal),[2] Protonotarios,[3] and Abate,[4] but several factors have prompted a reexamination. One is

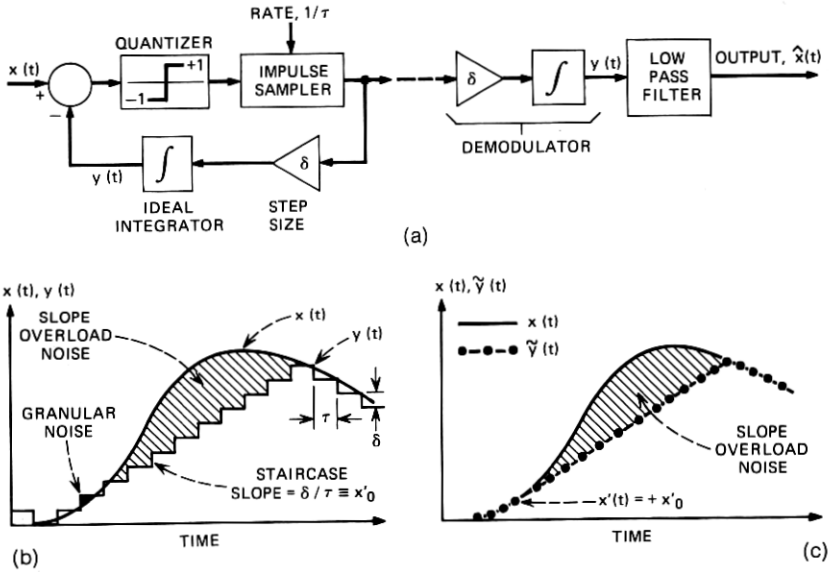

Fig. 1—Linear ΔM codec with perfect feedback integrator. (a) Equivalent block diagram. (b) Input and feedback signals. (c) Model used.

that some important disparities among the results of these separate studies remain unresolved; another is that the existing formulas do not, either individually or collectively, pertain to all slope-following capacities and input spectra; and finally, few explicit clues are available as to just how accurate each formula is and where it loses validity. In response to this situation, we have endeavored to find an expression for slope overload noise power that is accurate for all slope-following capacities and input spectra of possible interest. The result reported here satisfies that objective.

1.2 *Noise Descriptions and Definitions*

The idealized ΔM codec (coder/decoder) shown in Fig. 1 exemplifies the process we want to analyze: Every τ seconds the input signal ($x(t)$) is compared with a locally quantized version of itself ($y(t)$), and a unit impulse is generated with a polarity that is $\begin{pmatrix}\text{positive}\\ \text{negative}\end{pmatrix}$ if $\begin{pmatrix}x > y\\ x < y\end{pmatrix}$. The resulting binary impulse stream is applied through a feedback gain factor (δ) and ideal integrator to produce $y(t)$. At the decoder, $y(t)$ is reconstructed by using a replica

of the coder feedback network, and a final low-pass filter smooths the sharp edges of $y(t)$, yielding a closer approximation to $x(t)$.

Since $y(t)$ cannot change by more than δ units in τ seconds, δ/τ is the highest input signal rate-of-change that the ΔM codec can follow. We call δ/τ the ΔM *slope-following capacity* and denote it by x_o'. When $|dx/dt|$ exceeds this quantity, *slope overload* occurs and gives rise to the kind of error shown in Fig. 1b. In addition to this sporadic form of distortion, the "hunting" of $y(t)$ for $x(t)$ by means of quantum steps gives rise to a perpetual distortion called *granular noise*. Obviously, granular noise is reduced by decreasing δ, but at the expense of a reduced slope-following capacity and, hence, greater slope overload noise.

To delineate slope overload and granular noise for purposes of this analysis, let us suppose that $x(t)$ is passed first through a ΔM codec having infinitesimal δ and τ, but with the ratio between them the same as in the actual system (Fig. 1a). The decoded output (before the final filter) will then be the smooth function $\tilde{y}(t)$ shown in Fig. 1c. If $\tilde{y}(t)$ is then passed through the actual system, the decoded signal will be a very close approximation to $y(t)$, Fig. 1b. In agreement with previous conventions, we define slope overload noise to be the difference between $x(t)$ and $\tilde{y}(t)$; and the remaining distortion, $(\tilde{y}(t) - y(t))$, is defined to be granular noise. This essentially is the approach tacitly followed in most of the published literature on ΔM noise.[1-7]

We define a slope overload noise burst to be the nonzero difference between $x(t)$ and $\tilde{y}(t)$ over an interval $[t_a,t_b]$, which starts because $|dx/dt| > x_o'$ at $t = t_a$ and ends because $\tilde{y}(t)$ intersects $x(t)$ at $t = t_b$, (e.g., see Fig. 2, in which $t_a = 0$). The mean power of these bursts, averaged over all time, is the *slope overload noise power*.

Two qualitatively different kinds of noise bursts can be identified. One is the kind initiated when $|dx/dt|$ increases through x_o' while $\tilde{y}(t)$ is following $x(t)$, which we call *primary noise* (see Figs. 1c and 4b). The other arises when a prior burst terminates at a point where $|dx/dt|$ already exceeds x_o' (see Fig. 4c); the new burst that commences at this point we call *secondary noise*.

Finally, the *slope overload factor* is defined to be the ratio of the slope-following capacity to the rms input signal derivative, i.e.,

$$S \triangleq \frac{x_o'}{(dx/dt)_{\text{rms}}}. \tag{1}$$

It should be obvious that the noise power decreases monotonically

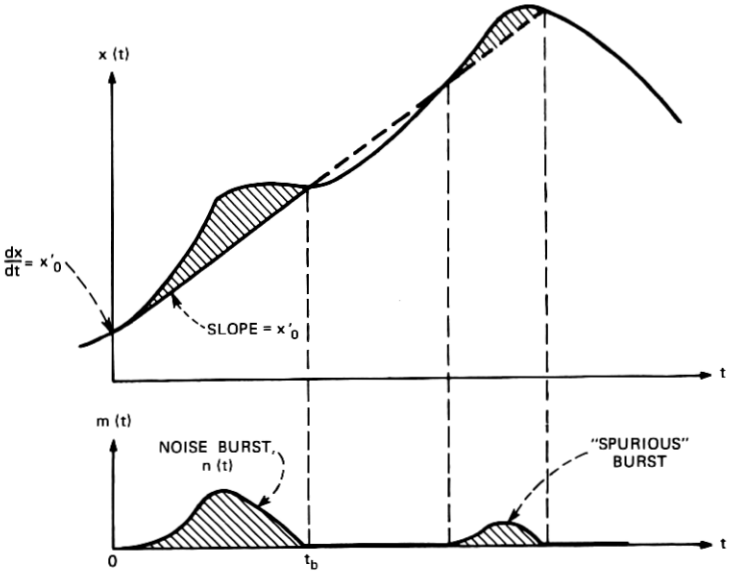

Fig. 2—Zetterberg's noise model.

with increasing S. It is also clear that when S is large (in which case $|dx/dt|$ rarely exceeds x_o'), secondary bursts are rare so that primary noise dominates the noise process; and that, by the same token, secondary noise dominates the noise process when S is small.

1.3 *Equivalent Input Process*

The generality of our analysis will be enhanced if we can assume that $\{x(t)\}$ is a bandlimited process. This assumption is made valid by regarding $\{x(t)\}$ as an equivalent process related to the true one as follows: Let the true input process be $\{x_o(t)\}$, having a power spectrum $X_o(f)$. Since the delta modulator really acts on discrete samples of the input separated by τ seconds, its response is the same as if the input were a process $\{x(t)\}$ having sample functions of the form

$$x(t) = \sum_{k=-\infty}^{\infty} x_o(k\tau) \frac{\sin(\pi(t - k\tau)/\tau)}{(\pi(t - k\tau)/\tau)} \tag{2}$$

and a power spectrum

$$X(f) = \sum_{n=-\infty}^{\infty} X_o\left(f + \frac{n}{\tau}\right); \qquad 0 \leqq f \leqq \frac{1}{2\tau} \text{ only.} \tag{3}$$

We will assume here that the sample function and slope overload noise depicted in Fig. 1c correspond to the bandlimited process $\{x(t)\}$, i.e., that the input spectrum is $X(f)$. If $\{x_o(t)\}$ is bandlimited by some frequency $W \leqq 1/(2\tau)$, the two processes, and consequently their spectra, are one and the same. (This condition is usually tacitly–though not always rightly–assumed in ΔM noise analyses.) If $\{x_o(t)\}$ is not so limited, the difference between the two processes is aliasing distortion, which can be analyzed separately.

1.4 *The Spectral Moments*

The spectral moments of the input process play a decisive role in establishing the past and present slope overload noise formulas. Following the convention of most authors, we define the nth moment to be

$$b_n = \int_0^\infty \omega^{2n} X(f) df. \tag{4}$$

The bandlimited nature of $X(f)$, as discussed above, guarantees the finiteness of all the moments. It is easy to show that the complete set of these finite moments, $(b_0, b_1, b_3, \cdots, b_n, \cdots)$, uniquely determines $X(f)$, just as the converse is true.

It should be obvious that b_n is the mean power of the nth derivative of $x(t)$, i.e., $b_n = \overline{(x^{(n)}(t))^2}$. Thus, for example, $\sqrt{b_1}$ is the rms derivative of the input and so (1) can be rewritten as

$$S = x_o'/\sqrt{b_1}. \tag{5}$$

Also, b_0 is nothing other than the input signal power, as distinct from the *ac* input power which we denote by σ^2. If the input contains no discrete dc component, then $b_0 = \sigma^2$; otherwise, b_0 exceeds σ^2 by the amount of the dc power.

Finally, we note from (4) that b_n is real and non-negative because $X(f)$ is. An additional relationship for b_n, derived by applying the Schwarz inequality to (4), is

$$b_n \geqq \frac{b_{n-1}^2}{b_{n-2}}; \qquad n \geqq 2, \tag{6}$$

that is, b_n for $n \geqq 2$ has a lower bound determined by the previous two moment values. We shall utilize this relationship later.

1.5 *Outline of the Work*

Our objective is to find a suitable approximation to the true slope overload noise power formula, the latter being denoted by $N(S)$. Section II describes the methods and results of previously published analyses. While the various approaches differ, they all suggest that this noise power is essentially determined by S and the first three spectral moments, b_0, b_1, and b_2. Section III treats this possibility as a premise and identifies a simple two-band process, the parameters of which can be chosen to yield any (b_0, b_1, b_2) and which can be analyzed precisely. The slope overload noise power for this process is derived and is denoted by $N_{tb}(S)$.

Unfortunately, $N_{tb}(S)$ is *not* precisely applicable to all spectra having the same b_0, b_1, and b_2. Instead, it is a lower-bound variation for all such spectra, which becomes increasingly unreliable in general as S decreases. To obtain a more universal estimate [denoted by $N_o(S)$] it is necessary to determine how much the slope overload noise power deviates from $N_{tb}(S)$ for spectra other than the two-band kind.

To this end, Section IV derives a noise power formula, $N_l(S)$, applicable to all spectra but confined to the large-S region ($S \geqq 3.5$), and Section V derives a noise power formula, $N_s(S)$, applicable to all spectra but confined to the small-S region ($S \approx 0$). Section VI then combines these results to obtain a two-region approximation, $N_o(S)$, which is accurate for all $X(f)$ and S. The result is given by (62) and (77), where α_1, α_2, a_1, a_2, a_3, and a_4 are related to the spectrum parameters b_0, b_1, b_2, b_3, b_4, b_5, $X(0)$, and $\int_o^\infty \omega^{-2}[X(f) - X(0)]df$. Further study shows that (77) alone can be used over all S with an accuracy of 1 dB or better up to $S = 6.5$, beyond which point $N(S)$ is at least 119 dB below the input signal power. For practical purposes, therefore, our final approximation to $N(S)$ is just (77), with a_1, a_2, a_3, and a_4 given by (72) through (75).

Section VII demonstrates the new result for two important families of spectra, and compares $N_o(S)$ with the noise power formula of Protonotarios. The latter is found to be highly accurate for most spectra of practical interest and $S \geqq 2.0$.

II. REVIEW OF PREVIOUS WORK

In the approaches of Zetterberg, Rice, and Protonotarios, $N(S)$ is approximated as the product of the mean energy ($\mathcal{E}$) per slope overload burst and the average rate of occurrence (R) of such bursts. A burst is assumed to commence whenever $|x'(t)|$ increases through

the value x'_o, which means that only primary noise is considered in these studies. The average rate of these events is known from the earlier work of Rice[8] to be

$$R = \frac{1}{\pi}\sqrt{\frac{b_2}{b_1}} \exp\{-(x'_o)^2/2b_1\}. \tag{7}$$

To find $\mathcal{E}$, Zetterberg uses the model shown in Fig. 2, where the solid line of slope x'_o represents the demodulator output for the duration of the burst, i.e., from $t = 0$ to $t = t_b$. Clearly, the noise is

$$n(t) = x(t) - [x(0) + x'_o t]; \qquad 0 \leqq t \leqq t_b \text{ only} \tag{8}$$

which is the first burst depicted in Fig. 2. To avoid deriving the random quantity t_b, Zetterberg regards the slope overload burst to be the entire excursion of $x(t)$ above the line $[x(0) + x'_o t]$, which is the variation $m(t)$ in Fig. 2 rather than just $n(t)$. This is obviously an approximation, since $m(t)$ can contain one or more spurious bursts that are not really part of the original noise burst, as seen. Such bursts, however, are low in both energy and probability of occurrence when $S \gg 1$.

Zetterberg proceeds by finding, at each t, the average of m^2 over the noise burst ensemble, and then integrating over all time and multiplying by R, (7). If done correctly, this leads to an estimate of $N(S)$ which is marred only by the inclusion of spurious burst contributions and the ignoring of secondary noise effects. In fact, however, Zetterberg errs in defining the initial conditions of the burst and in averaging over these conditions, leading to an incorrect solution.* In addition, Zetterberg makes a number of functional approximations and at least one algebraic error.* For all these reasons, his final result is incorrect and will not be repeated here.

The approach of Rice reverses that of Zetterberg, in that the energy per burst is found first and then averaged over the noise burst ensemble. The problem of spurious bursts is thus avoided, but at the expense of having to find t_b. Rice accomplishes this by expanding $x(t)$ into a power series about $t = 0$, and then ignoring fourth-order powers in t and higher, an approximation that gains in validity with increasing S. In addition, he approximates the third derivative of $x(t)$ at $t = 0$ by its conditional mean given that $x'(0) = x'_o$. This can be shown to be $-(b_2/b_0)x'_o$, and the relative variation of $x'''(0)$ about this value tends to be small when $S \gg 1$.

* See Protonotarios[3] for a discussion of these errors.

Using these two approximations, and correctly identifying and averaging over the initial conditions of the burst, Rice obtains the result

$$N_R(S) = \frac{243}{4\sqrt{2\pi}}\left(\frac{b_1^2}{b_2}\right)\frac{1}{S^5}\exp(-S^2/2). \tag{9}$$

Note that the ratio of noise power to signal power (b_0) depends solely on S and $\gamma \triangleq b_1^2/b_0b_2$. From (6) we see that $\gamma \leqq 1$ and observe that $\gamma = 1$ only for an infinitely narrowband spectrum.

It should also be noted that, as $S \to 0$, $N_R(S)$ increases without bound at a rate S^{-5}. This is clearly not a true representation since $N(S)$ should approach the ac signal power (σ^2) in the limit of zero slope-following capacity.*

Noting the disparity between Zetterberg's result and Rice's, even at large S where both should converge to exactness, Protonotarios has attempted to settle the issue by combining Zetterberg's more accurate model with Rice's correct averaging procedure. His analysis leads to a double integral solution which is exact except for the inclusion of spurious contributions and the ignoring of secondary noise effects. In reducing this formal result, Protonotarios makes some functional approximations and obtains the following:

$$N_P(S) = \frac{243}{4\sqrt{2\pi}}\left(\frac{b_1^2}{b_2}\right)\frac{1}{S^5}\exp(-S^2/2)A(\chi) \tag{10}$$

where

$$\chi = \frac{2^{5/8}}{3}S/(b_1^2/b_2b_0)^{1/8} \tag{11}$$

and $A(\cdot)$ is a function involving powers and exponentials of the argument, [eq. (66) of Ref. 3]. Once more, the ratio of noise power to signal power depends solely on S and γ. In the limit as $S \to \infty$, $A(\chi)$ approaches 1 and so $N_P(S)$ converges to Rice's result, $N_R(S)$. In the limit as $S \to 0$, $A(\chi)$ varies as S^4 so that $N_P(S)$ varies as S^{-1} rather than S^{-5}. This is still an unbounded increase, however, so that (10) is still not acceptable as a complete characteristic.

Abate's derivation of $N(S)$ follows an approach quite different from the others. Using simulation results reported by O'Neal[2] for three particular spectra, he has developed an empirical relationship between the ΔM sampling frequency and the slope overload factor for which

* If the input contains a discrete dc component, the delta modulator will follow it exactly so long as $S \neq 0$; hence the result $\lim_{S\to 0} N(S) = \sigma^2$.

granular-plus-slope overload noise power is minimized. Combining that relationship with a simplifying approximation to van de Weg's formula for granular noise power,[5] Abate obtains the following expression for slope overload noise power:

$$N_A(S) = \frac{8\pi^2}{27} \frac{b_1}{(2\pi W)^2} (1 + 3S) \exp(-3S) \tag{12}$$

where W is the signal truncation bandwidth.* We see that $N_A(S)$ goes to a finite value as $S \to 0$, and that its variation at large S is exponential; in both respects, it differs from $N_R(S)$ and $N_P(S)$. If we now define

$$K \triangleq \frac{8\pi^2}{27} \frac{b_2}{(2\pi W)^2 b_1}, \tag{13}$$

(12) reduces to the form

$$N_A(S) = K \left(\frac{b_1^2}{b_2}\right) (1 + 3S) \exp(-3S). \tag{14}$$

Evaluating K for the spectra studied by O'Neal, we find that it lies between 1.074 and 1.75 for the three cases, a range of just 2 dB. It is tempting to speculate, therefore, that (14) is a more correct form in general than (12), with K a universal constant on the order of unity, and that the apparent 2-dB spread in K over the three spectra is a result of experimental uncertainties. If we accept this notion, we again have the result that the ratio of noise power to signal power depends solely on S and γ.

III. NOISE POWER IN TERMS OF b_0, b_1, b_2

3.1 *The Two-Band Process*

The published results cited above suggest that $N(S)$ is essentially the same for all processes having the same values for the zeroth, first, and second moments. Assuming for the present that this supposition is correct, we call attention to the two-band process, the spectrum of which is shown in Fig. 3a. In the limit as the two bands become infinitely narrow, the zeroth, first, and second moments become precisely b_0, b_1, and b_2. By analyzing this simple process, therefore, we can derive an exact noise power formula $[N_{tb}(S)]$ in terms of b_0, b_1, and b_2 and then see how universal it really is.

* The three spectra treated by O'Neal are of the truncated Butterworth type, with corner frequency-to-bandwidth ratios of 0.068, 0.25, and ∞. The data used to derive (12) cover an S-range from about 1.4 to 4.2.

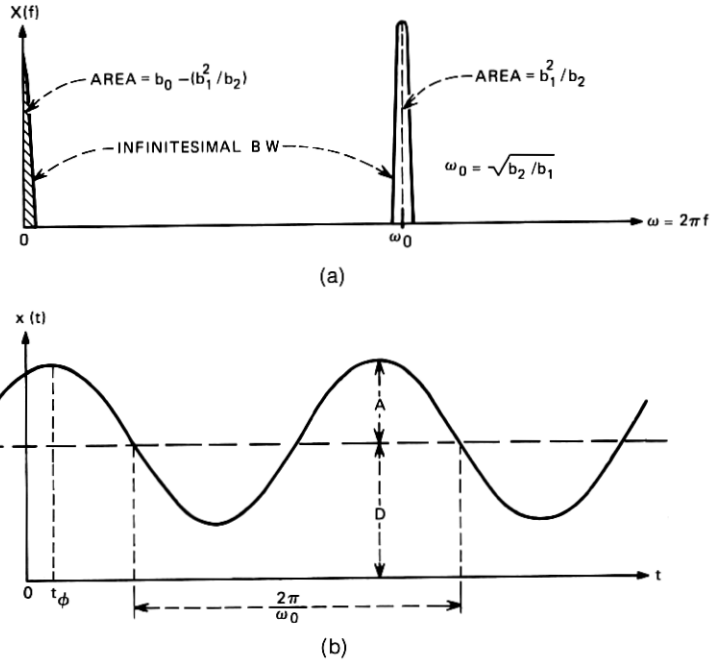

Fig. 3—The two-band random process. (a) Power spectrum. (b) Sample function.

To appreciate the simplicity of the two-band process for purposes of analysis, we should view it in the time domain. A sample function is shown in Fig. 3b and is seen to consist of a dc level, D, plus a sinusoid having radian frequency $\omega_o = \sqrt{b_2/b_1}$, phase $\phi = \omega_o t_\phi$, and amplitude A. D is a Gaussian variate, whose mean and variance across the sample function ensemble are 0 and $(b_0 - b_1^2/b_2)$, respectively; ϕ is a uniformly distributed variate on $[-\pi, +\pi]$; A is a Rayleigh variate of mean-square value $2b_1^2/b_2$; and D, ϕ, and A are mutually independent.

We can derive the slope overload noise power for this process by finding the mean noise power associated with a given sample function and averaging over the distributions on D, ϕ, and A. This approach is simplified by the fact that D and ϕ do not really influence the result. That is, the noise pattern for a given sample function converges ultimately to a variation about D that depends solely on the sinewave amplitude and frequency (Fig. 4).

We thus see that the noise power per sample function is the steady-state noise energy per half-cycle, denoted by $\mathcal{E}(A)$, times the rate of

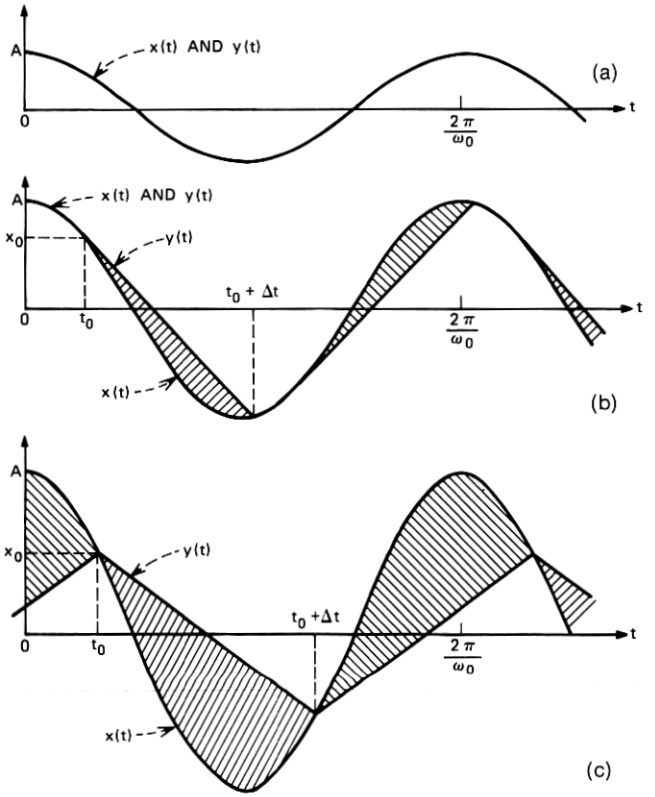

Fig. 4—The three regions of sinewave amplitude. (a) $0 \leqq A \leqq x_o'/\omega_o$ (no noise). (b) $(x_o'/\omega_o) < A < (x_o'/\omega_o)\sqrt{1 + \pi^2/4}$ (primary noise). (c) $A \geqq (x_o'/\omega_o)\sqrt{1 + \pi^2/4}$ (secondary noise).

occurrence of half-cycles, which is $\sqrt{b_2/b_1}/\pi$. The total noise power for the two-band process is then the average of this quantity over the distribution on A, i.e.,

$$N_{tb} = \frac{1}{\pi}\sqrt{\frac{b_2}{b_1}}\int_0^\infty \mathcal{E}(A)\underbrace{p(A)}_{(\text{pdf of } A)}dA\,. \tag{15}$$

Since A is known to be a Rayleigh variate of mean-square value $(2b_1^2/b_2)$, the only unknown is the energy function $\mathcal{E}(A)$.

3.2 *Derivation of* $\mathcal{E}(A)$

Three distinct regions of A can be identified, each giving rise to a distinct pattern of signal and noise. The region depicted in Fig. 4a

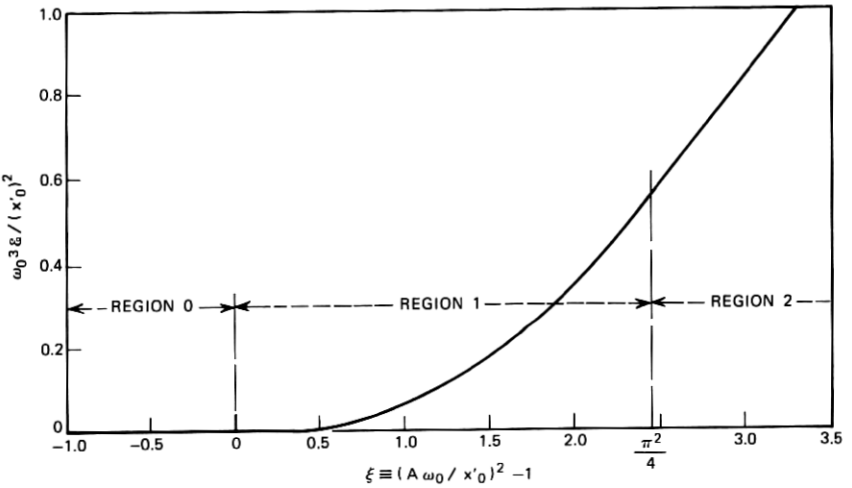

Fig. 5—Noise energy per half-cycle as a function of A.

(Region 0) is one in which no slope overload occurs because $|x'(t)| < x'_o$ at all t. Clearly, $\mathcal{E}(A) = 0$ in this case. The region depicted in Fig. 4b (Region 1) is one in which slope overload occurs in each half-cycle, but over less than the complete interval. We see that the noise in this case is primary noise, as defined earlier. Finally, the region depicted in Fig. 4c (Region 2) is one in which slope overload occurs for the entire duration of each half-cycle. The noise in this case is seen to be secondary noise.*

To find $\mathcal{E}$ in Region 1, we analyze the burst spanning $[t_o, t_o + \Delta t]$ in Fig. 4b. The noise energy in this burst is

$$\mathcal{E} = \int_{t_o}^{t_o+\Delta t} [A \cos \omega_o t - \{x_o - x'_o(t - t_o)\}]^2 dt. \tag{16}$$

The quantities x_o and t_o are found by means of trigonometric identities to be

$$x_o = \sqrt{A^2 - (x'_o/\omega_o)^2} \quad \text{and} \quad t_o = \frac{1}{\omega_o} \sin^{-1}\left(\frac{x'_o}{A\omega_o}\right). \tag{17}$$

Unfortunately, the quantity Δt cannot be solved for explicitly, but is

* For the special process under discussion, we see that a given sample function has either no noise at all, primary noise only, or secondary noise only. For more spectrally distributed processes, both kinds of noise occur in the same sample function and in a less regular pattern.

related to A by the transcendental equation

$$\left[\frac{\omega_o\Delta t - \sin(\omega_o\Delta t)}{1 - \cos(\omega_o\Delta t)}\right]^2 = \left(\frac{A\omega_o}{x_o'}\right)^2 - 1 \triangleq \xi. \tag{18}$$

We can relate $\mathcal{E}$ to A (or ξ) by combining (16), (17), and (18) and eliminating the common parameter, $\omega_o\Delta t$, between (16) and (18). The result is a unique correspondence between $\omega_o^3\mathcal{E}/(x_o')^2$ and ξ having the variation shown in Fig. 5 for Region 1. (Note that Region 1 corresponds to the ξ-interval $[0, \pi^2/4]$.) A highly accurate functional description of this variation has been found to be

$$\frac{\omega_o^3\mathcal{E}}{(x_o')^2} = \frac{81}{140\pi}\xi^{7/2}[0.43\exp(-0.5014\xi) + 0.57\exp(-2.10\xi)]; \quad 0 \leqq \xi < \pi^2/4. \tag{19}$$

Comparison with exact results shows this function to be accurate to within 0.8 percent.

To find $\mathcal{E}$ in Region 2, we analyze the burst spanning $[t_o, t_o + \Delta t]$ in Fig. 4c. In this case, x_o and t_o are given by (17), as before, but $\omega_o\Delta t$ is precisely π for all A. Applying these relationships to (16) and performing the indicated integration, we obtain

$$\frac{\omega_o^3\mathcal{E}}{(x_o')^2} = \frac{1}{2}\left[\xi - \left(3 - \frac{\pi^2}{6}\right)\right]; \qquad \xi \geqq \pi^2/4. \tag{20}$$

This variation is also shown in Fig. 5.

3.3 *Expression for $N_{tb}(S)$*

We now have expressions for $\mathcal{E}$ in the three regions of A and can average this complete result over the distribution on A (or ξ) to find N_{tb}, (15). By using (18), along with $\omega_o^2 = b_2/b_1$, $S = x_o'/\sqrt{b_1}$, and the fact that A is a Rayleigh variate of mean-square value $(2b_1^2/b_2)$, we obtain

$$p(\xi) = \frac{S^2}{2}\exp\left(-\frac{S^2}{2}\right)\exp\left(-\frac{S^2}{2}\xi\right); \qquad \xi \geqq -1$$
$$= 0; \qquad \text{elsewhere.} \tag{21}$$

Combining this with (15), (19), and (20), we obtain

$$N_{tb}(S) = \underbrace{\left(\frac{b_1}{b_2}\right)^2 F_1(S)}_{\substack{\text{Primary}\\ \text{Noise}}} + \underbrace{\left(\frac{b_1}{b_2}\right)^2 F_2(S)}_{\substack{\text{Secondary}\\ \text{Noise}}} = \left(\frac{b_1}{b_2}\right)^2 F(S) \tag{22}$$

where $F(S) \triangleq F_1(S) + F_2(S)$, and

$$F_1(S) = \frac{81}{560}\left(\frac{\pi}{2}\right)^8 S^4 \exp\left(-\frac{S^2}{2}\right)\left[0.43Q\left\{\frac{\pi^2}{4}\left(\frac{S^2}{2}+0.5014\right)\right\} + 0.57Q\left\{\frac{\pi^2}{4}\left(\frac{S^2}{2}+2.10\right)\right\}\right]; \quad (23)$$

$$F_2(S) = \left[1+\left(\frac{5\pi^2-36}{24}\right)S^2\right]\exp\left\{-\left(1+\frac{\pi^2}{4}\right)\frac{S^2}{2}\right\}; \quad (24)$$

$$Q\{u\} = \frac{1}{u^{9/2}}\left\{\frac{105\sqrt{\pi}}{16}\operatorname{erf}(\sqrt{u}) - \left[u^{7/2}+\frac{7}{2}u^{5/2}+\frac{35}{4}u^{3/2}+\frac{105}{8}u^{1/2}\right]\exp(-u)\right\}. \quad (25)$$

The variation $F(S)$ is shown in Fig. 6 along with its component parts, $F_1(S)$ and $F_2(S)$. These curves indicate, for the two-band process, which region of S is dominated by primary noise and which region by secondary noise.

The only inexactness in our result for $N_{tb}(S)$ arises from the functional fit to $\mathcal{E}$ in Region 1, (19). Since this fit is accurate to within ± 0.8 percent at all ξ, and both $\mathcal{E}(\xi)$ and $p(\xi)$ are non-negative func-

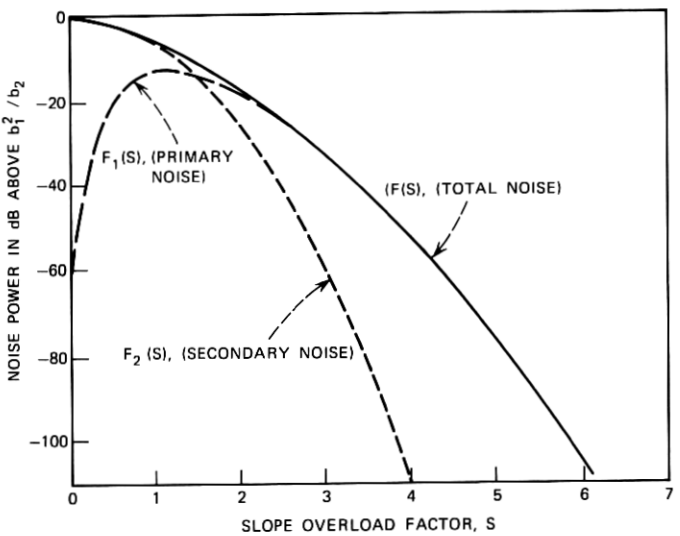

Fig. 6—Normalized noise powers for the two-band process.

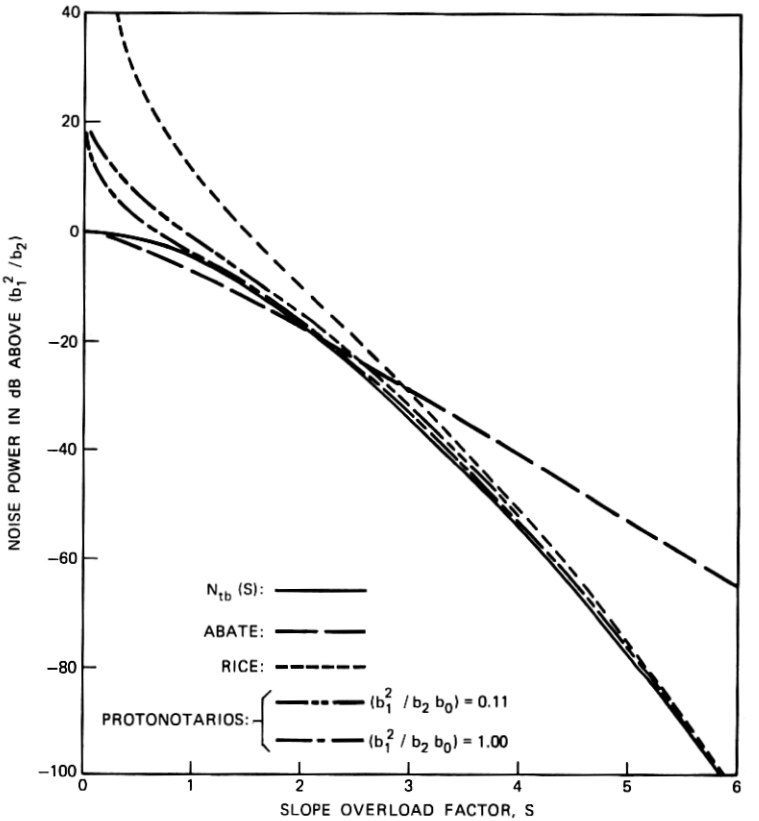

Fig. 7—Comparison of $N_{tb}(S)$ with previous results.

tions, the given expression for $N_{tb}(S)$ is also accurate to within ± 0.8 percent (or ± 0.035 dB).

3.4 *Comparisons and Interpretations*

The variation of N_{tb} with S is plotted in Fig. 7, along with the variations of N_R, (9); N_P, (10); and N_A, [(14) with $K = 1$]. Of particular interest is the fact that $N_{tb}(S)$ converges with the results of Rice and Protonotarios as $S \to \infty$. The approximations underlying the analyses of Rice and Protonotarios become increasingly valid as S increases, so the convergence of $N_{tb}(S)$ with their results is not surprising. The apparent dependence of noise power on the moments b_1 and b_2 alone at large S is explained by the fact that slope overload bursts are of

short duration in this region; hence, they are shaped primarily by the lower-order curvature of $x(t)$, which is reflected in b_1 and b_2. As S decreases towards small values, however, the higher-order curvature of $x(t)$, reflected in b_3, b_4, etc., also influences the noise bursts and, consequently, the noise power. We should therefore expect the true noise power $[N(S)]$ associated with a given spectrum to reflect other features of that spectrum at low S besides b_1 and b_2. If this is so, then $N_{tb}(S)$ cannot be assumed to be a universal formula.

To show that this expectation is correct, we note that, as $S \to 0$, N_{tb} converges to b_1^2/b_2, which is precisely the ac power (σ^2) in the two-band process. This is a quite general result, i.e., $N(S)$ always converges to σ^2 as $S \to 0$. However, some other process having the same b_0, b_1, and b_2 can have an ac power anywhere between b_1^2/b_2 and b_0, so that $N(S)$ will not converge to b_1^2/b_2 for all spectra having these moments in common.

We conclude, then, that $N(S)$ and $N_{tb}(S)$ converge at high S but become increasingly dissimilar as S decreases towards zero, the dissimilarity depending on the differences between the actual process spectrum and the two-band spectrum having the same b_0, b_1, and b_2. In Part 2 (following), we will derive a factor which relates $N_{tb}(S)$ and $N(S)$ when $X(f)$ is not a two-band spectrum.

Part 2

IV. NOISE POWER FOR $S \geqq 3.5$

We now derive a noise power formula applicable to all spectra, with S large (primary noise only). The derivation combines the power series method of Rice with the infinite-time averaging procedure used by Zetterberg and Protonotarios. The differences here are that many terms of the power series expansion are included, and steps are taken to minimize the contributions from spurious bursts. The complicated expression that results is reduced to a simple formula $[N_l(S)]$ that displays explicitly the influence of the higher-order spectral moments.

4.1 *Power Series Representation of the Noise Burst*

Let $t = 0$ be the time origin of a particular positive-going burst, so that $x'(0) = x_o'$ and $x''(0) > 0$, e.g., Fig. 2. Beginning at $t = 0$, $\bar{y}(t)$ follows the straight line $x(0) + x_o't$ until this ramp function intersects $x(t)$ again. We can therefore define the quantity

$$v(t) \triangleq x(t) - [x(0) + x'_o t]; \qquad t > 0 \tag{26}$$

and write the variation of the noise burst as

$$\begin{aligned} n(t) &= v(t) \quad \text{if } v(t') > 0 \quad \text{for all} \quad 0 < t' \leqq t \\ &= 0 \quad \text{otherwise.} \end{aligned} \tag{27}$$

Henceforth, we shall use the symbols n_t and v_t to denote $n(t)$ and $v(t)$, respectively.

Following Rice, we can express $x(t)$ by a power series expansion about $t = 0$. Noting that $x'(0) = x'_o$ and denoting $x''(0)$ by x''_o, v_t can be written as

$$v_t = \tfrac{1}{2}x''_o t^2 + \frac{1}{3!}x'''(0)t^3 + \cdots \frac{1}{m!}x^{(m)}(0)t^m + \cdots. \tag{28}$$

We now invoke the property of Gaussian random processes that the mth and $(m-2)$th derivatives at a given time instant are related by

$$x^{(m)} = -\frac{b_{m-1}}{b_{m-2}}x^{(m-2)} + d_m \tag{29}$$

where d_m is a zero-mean Gaussian variate of mean-square value

$$\overline{d_m^2} = b_m - \frac{b_{m-1}^2}{b_{m-2}}. \tag{30}$$

With this relationship we can write v_t as follows:

$$\begin{aligned} v &= \left\{x''_o\left[\frac{t^2}{2!} - \frac{b_3}{b_2}\frac{t^4}{4!} + \frac{b_3}{b_2}\cdot\frac{b_5}{b_4}\frac{t^6}{6!} - \cdots\right]\right. \\ &\quad \left. - x'_o\left[\frac{b_2}{b_1}\frac{t^3}{3!} - \frac{b_2}{b_1}\cdot\frac{b_4}{b_3}\frac{t^5}{5!} + \frac{b_2}{b_1}\cdot\frac{b_4}{b_3}\cdot\frac{b_6}{b_5}\frac{t^7}{7!} - \cdots\right]\right\} \\ &\quad + \left\{d_3\frac{t^3}{3!} + d_4\frac{t^4}{4!} - \left[\frac{b_4}{b_3}d_3 - d_5\right]\frac{t^5}{5!} - \left[\frac{b_5}{b_4}d_4 - d_6\right]\frac{t^6}{6!} + \cdots\right\} \\ &\triangleq A_t + \delta_t \end{aligned} \tag{31}$$

where A_t is the first bracketed quantity and δ_t is the second. We see that A_t is the conditional mean of v_t given that $x'(0) = x'_o$ and $x''(0) = x''_o$; and that δ_t is a linear sum of mutually independent zero-

mean Gaussian variates (d_3, d_4, etc.) whose mean-square value at time t is therefore

$$\overline{\delta_t^2} \equiv \sigma_t^2 = \left[\left(\frac{t^3}{3!} - \frac{b_4}{b_3}\frac{t^5}{5!} + \cdots\right)^2 \overline{d_3^2} + \left(\frac{t^4}{4!} - \frac{b_5}{b_4}\frac{t^6}{6!} + \cdots\right)^2 \overline{d_4^2} + \cdots\right]. \quad (32)$$

We thus have the result that the conditional pdf of v at time t is

$$p\{v_t | x_o', x_o''\} = \frac{1}{\sqrt{2\pi}\sigma_t} \exp\left\{-\frac{1}{2}\left(\frac{v_t - A_t}{\sigma_t}\right)^2\right\}. \quad (33)$$

4.2 *Derivation of Mean Noise Power*

Let $\overline{n_t^2}$ be the conditional mean square value of n at time t, given that $x'(0) = x_o'$ and $x''(0) \equiv x_o'' > 0$. To find the mean burst energy when $x'(0) = x_o'$, we must average $\overline{n_t^2}$ with respect to x_o'' and integrate the result over all time. We can then multiply this mean energy by the mean rate of primary noise burst occurrences to obtain the mean noise power. This approach is valid so long as secondary noise can be neglected, which it can in the region $S \geqq 3.5$ under consideration.

From Protonotarios,[3] we know that the correct density function for averaging with respect to the conditions $x'(0) = x_o'$ and $x_o'' > 0$ is

$$p(x_o'') = \frac{x_o''}{b_2} \exp\left\{-\frac{(x_o'')^2}{2b_2}\right\}; \qquad x_o'' \geqq 0 \quad (34)$$

while from Rice[8] we know that the mean rate of noise burst occurrences is $(\sqrt{b_2/b_1}/\pi) \exp(-S^2/2)$. The noise power in the region $S \geqq 3.5$ can thus be accurately given by

$$N(S) = \frac{1}{\pi}\sqrt{\frac{b_2}{b_1}} \exp\left(-\frac{S^2}{2}\right) \int_0^\infty \int_0^\infty \frac{x_o''}{b_2} \cdot \exp\left\{-\frac{(x_o'')^2}{2b_2}\right\} \overline{n_t^2(x_o', x_o'')} dx_o'' dt. \quad (35)$$

The remaining analytical task is to find $\overline{n_t^2(x_o', x_o'')}$.

The method of Protonotarios in this regard amounts to averaging v_t^2 over positive values using the conditional pdf of v_t, (33). To do this, however, is to incur the spurious burst problem depicted by Fig. 8a. The following line of reasoning leads to an improved procedure.

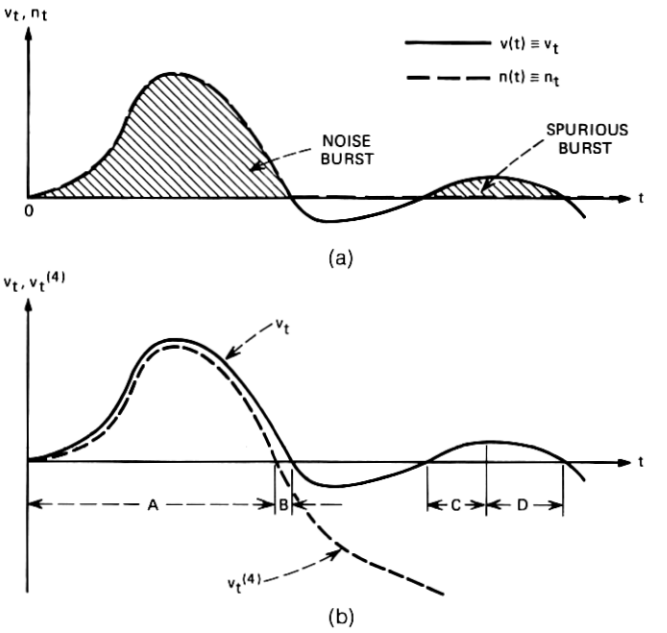

Fig. 8—An illustration of v_t and n_t. (a) v_t and n_t. (b) v_t and $v_t^{(4)}$.

Let $A_t^{(4)}$ denote the partial power series for A_t up to and including the fourth-order term, and let

$$v_t^{(4)} \equiv A_t^{(4)} + \delta_t. \tag{36}$$

We can show that $v_t^{(4)} \approx v_t$ when t is small and that $v_t > v_t^{(4)}$ in general. What we have found in particular is that, for S greater than about 2, the difference between v_t and $v_t^{(4)}$ does not widen appreciably over a typical burst duration (see Fig. 8b). Also, since $A_t^{(4)}$ is a strongly decreasing function of t beyond its peak, $v_t^{(4)}$ tends to be the same.

We therefore calculate $\overline{n_t^2}$ according to the following criterion: A given value of v_t is counted as part of the noise (i.e., n_t is assumed to be v_t) if either $\{v_t > 0, v_t^{(4)} > 0\}$ or $\{v_t > 0, v_t^{(4)} < 0, \dot{v}_t < 0\}$;* otherwise, v_t is not counted and n_t is assumed to be 0. For the sample function shown in Fig. 8b, this means that the energies in intervals A and B are both counted in the calculation of $\overline{n_t^2}$; the energy in interval C is not counted, since $v_t^{(4)} < 0$ and $\dot{v}_t > 0$; and the energy in interval D is counted, even though it is clearly spurious. We can reduce contribu-

* The symbol $\dot{v}_t$ stands for $dv(t)/dt$.

tions of the latter type, however, by using a suitably finite upper limit in the integration over time in (35). That is, we choose an upper limit sufficiently high that virtually all legitimate noise contributions are counted in the calculation but sufficiently low that some spurious contributions are omitted. By studying the time variations of A_t and δ_t under a wide variety of conditions, we have settled on an upper time limit of $3.5\sqrt{b_1/b_2}$.

Using the above criterion, we have been able to show that

$$\overline{n_t^2} = \frac{\sigma_t^2}{2}\left\{(1+2\alpha^2)[1+\operatorname{erf}(\alpha_4)] + \frac{2}{\sqrt{\pi}}(2\alpha-\alpha_4)\exp(-\alpha_4^2)\right\} + \frac{\sigma_t^2}{4}(\operatorname{erfc}(\dot{\alpha}))\left\{(1+2\alpha^2)[\operatorname{erf}(\alpha)-\operatorname{erf}(\alpha_4)] + \frac{2}{\sqrt{\pi}}[\alpha\exp(-\alpha^2)-(2\alpha-\alpha_4)\exp(-\alpha_4^2)]\right\} \quad (37)$$

where:

$$\alpha \triangleq A_t/\sqrt{2\sigma_t^2}; \quad (38)$$

$$\alpha_4 \triangleq A_t^{(4)}/\sqrt{2\sigma_t^2}; \quad (39)$$

and

$$\dot{\alpha} \triangleq \dot{A}_t/\sqrt{2\overline{(\dot{\delta}_t)^2}}. \quad (40)$$

To complete the derivation of $N(S)$, we insert this complicated expression into (35) and perform the integrations over x_o'' and t, remembering to use an upper limit of $3.5\sqrt{b_1/b_2}$ in the time integral.

4.3 *Simplified Formula*

The formal solution just described is believed to be more exact than that of Protonotarios [eq. (53) of Ref. 3], because it entails a substantial reduction in the spurious burst contributions. Furthermore, in reducing his formal solution to computation, Protonotarios makes a number of functional approximations which obscure the influence of the higher-order moments b_3, b_4, etc. In reducing the present solution to computation, we must also make approximations but of a different kind, i.e., those associated with performing numerical double integration and truncating the infinite power series in the integrand. The impact of the higher-order moments, however, is not approximated away in the process; in fact, the following discussion develops an empirical expression [denoted by $N_I(S)$] which exhibits these influences explicitly.

We define a dimensionless quantity, which we call the nth-moment excess, as

$$M_n \triangleq \frac{b_n - (b_{n-1}^2/b_{n-2})}{(b_2^{n-1}/b_1^{n-2})}; \qquad n \geqq 3. \tag{41}$$

From (6) we know that $M_n \geqq 0$ for all $n \geqq 3$ and, using Fig. 3, we can show that $M_n = 0$ for all $n \geqq 3$ if and only if $X(f)$ is the two-band spectrum. We can therefore say that $N(S)$ differs from $N_{tb}(S)$ only to the extent that M_3, M_4, etc., are not zero. A simple model that reflects this fact is one which describes the logarithmic difference between N and N_{tb} as a linear combination of the moment excesses,

$$\ln(N/N_{tb}) = AM_3 + BM_4 + CM_5 + \cdots \tag{42}$$

where the coefficients A, B, etc., are, in general, functions of S. To the extent that this representation is accurate, it is reasonable to assume further that the higher-order terms, involving M_6, M_7, etc., are negligible for $S \geqq 3.5$. The reason is that these moment excesses have little influence on slope overload bursts at such high slope-following capacities. The result of this line of reasoning is an approximation of the form

$$N(S \geqq 3.5) \doteq N_{tb}(S) \exp\{A(S)M_3 + B(S)M_4 + C(S)M_5\} \triangleq N_t(S). \tag{43}$$

We have tested this approximation by applying the double integral solution for $N(S)$, (35) and (37), to a number of spectra, using a ninth-order power series to represent v_t. With the computed noise powers for these spectra, we have then obtained results for $A(S)$, $B(S)$, and $C(S)$ over the range $3.5 \leqq S \leqq 10.0$ (Fig. 9) which appear to be quite accurate. In particular, the use of (43) with these results is found to predict $N(S \geqq 3.5)$, as computed from (35), to within 0.2 dB for all spectra of practical interest.

There exist, however, special conditions on $X(f)$ for which (43) yields too high estimates of the true noise power. This can occur when $X(f)$ contains an isolated high-frequency component which contributes materially to b_3, b_4, and/or b_5 but not to b_0, b_1, or b_2. Under such circumstances, $x(t)$ might change too rapidly during the noise bursts to be properly analyzed by the power series approach as used here. Calculations indicate that these cases fall outside the range of practical interest, so we need not consider them further.

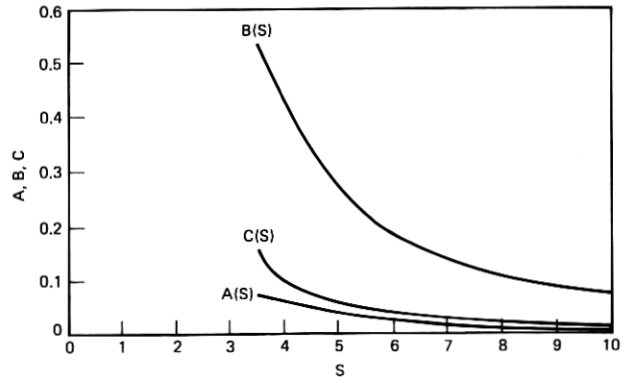

Fig. 9—Empirical results for A, B, and C; $S \geqq 3.5$.

V. NOISE POWER FOR $S \approx 0$

We now derive another noise power formula applicable to all spectra, but with S very small (secondary noise only). The representation we seek is a partial power series of the form

$$N(S \approx 0) \doteq \sigma^2[C_0 + C_1 S + C_2 S^2)] \triangleq N_s(S) \tag{44}$$

where σ^2 is the ac power of the input process.

5.1 *Formulation*

The analysis assumes $\{x(t)\}$ to be just the ac part of the input process, so that $\overline{x^2(t)} = \sigma^2$. Since dc components have no effect on noise power for $S \neq 0$, we are justified in ignoring them.

We consider x_o' to be so small compared to $\sqrt{b_1}$ (i.e., S so small compared to unity) that the delta modulator is always in slope overload. In this case, the decoded output [denoted here by $y(t)$ rather than $\bar{y}(t)$] is just a succession of alternating ramps of slope $\pm x_o'$, the slope polarity reversing whenever $y(t)$ intersects $x(t)$. This situation is illustrated in Fig. 10b. A valid model of the delta modulator for analyzing this case is given by Fig. 10a (cf. Ref. 9), from which we see that the noise signal is

$$n(t) = x(t) - y(t) = x(t) - x_o' \int_{-\infty}^{t} n_q(u)du \tag{45}$$

where

$$n_q(\cdot) \triangleq \operatorname{sgn}\{n(\cdot)\}. \tag{46}$$

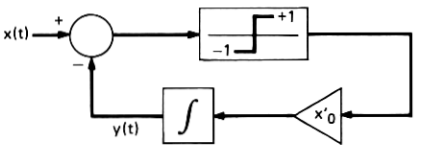

(a)

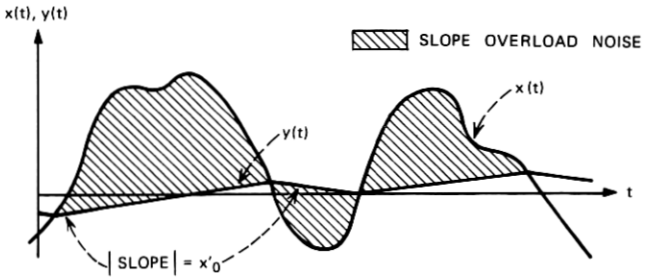

(b)

Fig. 10—Equivalent delta modulator and signals for $S \approx 0$. (a) ΔM model for $S \approx 0$. (b) Input and feedback signals.

The noise power in the region $S \approx 0$ can thus be accurately given by

$$N(S) = \overline{x^2(t)} - \underbrace{2x'_o\overline{\left[x(t)\int_{-\infty}^{t} n_q(u)du\right]}}_{-2\overline{x(t)y(t)}} + \underbrace{(x'_o)^2\overline{\int_{-\infty}^{t}\int_{-\infty}^{t} n_q(u)n_q(v)dudv}}_{\overline{y^2(t)}}. \quad (47)$$

If we envision each of these three terms as a power series in x'_o, we see that $\overline{x^2(t)}$ has a zero-order term only (i.e., is independent of x'_o); $-2\overline{x(t)y(t)}$ may contain first-, second-, and higher-order terms; and $\overline{y^2(t)}$ may contain second-order terms and higher. We can thus rewrite (47) as

$$N(S) = \underbrace{K_0}_{\overline{x^2(t)}} + \underbrace{[K_1x'_o + K_{2a}(x'_o)^2 + \cdots]}_{\overline{-2x(t)y(t)}} + \underbrace{[K_{2b}(x'_o)^2 + \cdots]}_{\overline{y^2(t)}}. \quad (48)$$

Retaining only terms up to second-order, substituting $x'_o = S\sqrt{b_1}$, and

comparing with (44), we see that

$$C_0 = \frac{K_0}{\sigma^2}; \qquad C_1 = \frac{K_1\sqrt{b_1}}{\sigma^2}; \qquad C_2 = \frac{(K_{2a} + K_{2b})b_1}{\sigma^2}. \tag{49}$$

Clearly, $K_0 = \overline{x^2(t)} = \sigma^2$, so that $C_0 = 1$ in all cases. The remainder of this section is devoted to finding C_1 and C_2.

5.2 *Derivation of* C_1

We will derive C_1 by evaluating the first-order term of $-2\overline{x(t)y(t)}$, (47), and then invoking (49). For x_o' very small, $n_q(t)$ does not differ appreciably from $x_q(t) \equiv \text{sgn}\{x(t)\}$, which is the quantizer response to $x(t)$ applied alone. It is therefore fruitful to represent $n_q(t)$ as

$$n_q(t) = x_q(t) + \theta(t) \tag{50}$$

where $\theta(t)$ is a correction signal related to the finiteness of x_o' and is defined by

$$\theta = \begin{cases} +2 & \text{if } y < x < 0 \\ -2 & \text{if } y > x > 0 \\ 0 & \text{otherwise.} \end{cases} \tag{51}$$

The relationships between $n_q(t)$, $x_q(t)$, and $\theta(t)$ are illustrated in Fig. 11. Although the peak magnitude of $\theta(t)$ is fixed, its "duty cycle" can be seen to depend directly on x_o'.

Inserting (50) into the cross term of (47) and interchanging the order of integration and averaging yields

$$-2\overline{x(t)y(t)} = -2x_o' \int_{-\infty}^{t} \overline{x(t)x_q(u)}du - 2x_o' \int_{-\infty}^{t} \overline{x(t)\theta(u)}du. \tag{52}$$

Since the duty cycle of $\theta(t)$ vanishes as $x_o' \to 0$, we can see that the first term must be identical to K_1x_o' in (48), while the second term contains $K_{2a}(x_o')^2$ plus higher-order terms in x_o'.

To evaluate the first term, we use a relationship applicable to $\{x(t)\}$ because it is a Gaussian process, namely,

$$\overline{x(t)x_q(u)} = \sqrt{\frac{2}{\pi}}\frac{\overline{x(t)x(u)}}{\sigma} = \sqrt{\frac{2}{\pi}}\frac{R_x(t-u)}{\sigma} \tag{53}$$

where $R_x(\tau)$ is the autocorrelation function of $\{x(t)\}$. We now apply this to the first term of (52) and use the fact that the area under $R_x(\tau)$ from $\tau = 0$ to $\tau = \infty$ is $\frac{1}{4}X(0)$. Equating the result to K_1x_o'

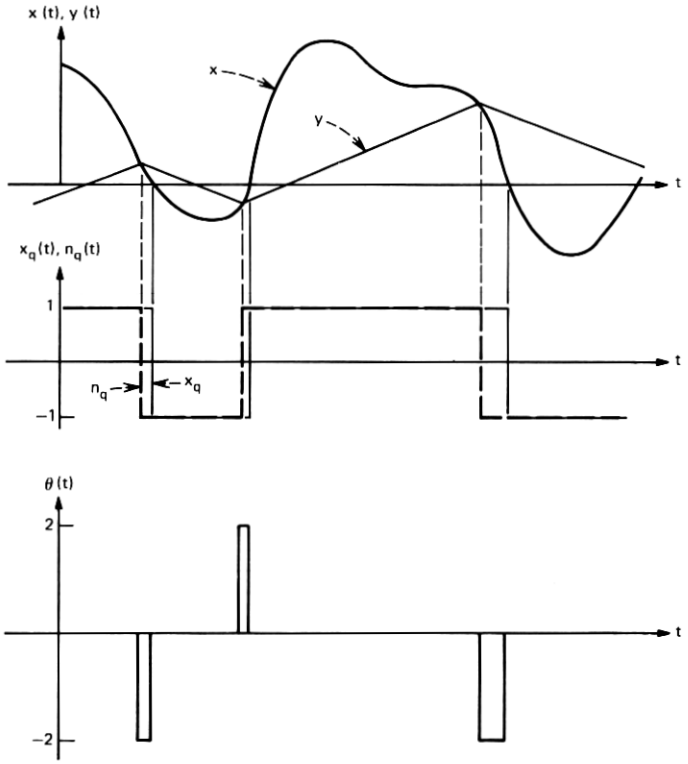

Fig. 11—The relationships between $x(t)$, $y(t)$, $x_q(t)$, $n_q(t)$, and $\theta(t)$.

we obtain

$$K_1 = -\frac{1}{\sqrt{2\pi}} \frac{X(0)}{\sigma} \tag{54}$$

which, from (49), yields

$$C_1 = -\frac{1}{\sqrt{2\pi}} \left[\frac{X(0)\sqrt{b_1}}{\sigma^3} \right]. \tag{55}$$

5.3 *Derivation of C_2*

The general approach used in the preceding analysis was also applied to finding C_2. Unfortunately, it leads to an approximation which is both highly complicated and not sufficiently precise for many spectra. For this reason, we have resorted to finding C_2 for a not-quite-Gaussian process having the same spectrum as the specified Gaussian one, and verifying that it is virtually exact under what appear to be "worst-

case" conditions. The details, which are documented but not published,[10] are quite involved and so we shall merely outline the approach.

Consider a wide sense stationary process $\{\tilde{x}(t)\}$ having sample functions of the form

$$\tilde{x}(t) = A \cos(\tilde{\omega}t + \phi) \tag{56}$$

where A is a Rayleigh-distributed amplitude of mean-square value $2\sigma^2$; ϕ is a random phase uniformly distributed over $[-\pi, +\pi]$; and $\tilde{\omega}$ is a random frequency whose pdf is

$$p(\tilde{\omega}) = \frac{1}{2\sigma^2} X(f = |\tilde{\omega}|/2\pi); \qquad \text{all } \tilde{\omega}. \tag{57}$$

It can be shown that the power spectrum for this process is $X(f)$, and that the ensemble pdf of $\tilde{x}$ at any t is Gaussian with zero mean and variance σ^2. Thus, $\{\tilde{x}(t)\}$ has certain properties in common with the Gaussian process $\{x(t)\}$ having the spectrum $X(f)$.

We can derive the mean slope overload noise power for the process $\{\tilde{x}(t)\}$ by finding the noise power for a single sample function, (56), and averaging over the distributions on A, ϕ, and $\tilde{\omega}$. Using the methods of Section III, we can show that the averaging over A and ϕ yields

$$\tilde{N}(x_o' \mid \tilde{\omega}) = \tfrac{1}{2}\overline{A^2} F\left(\frac{\sqrt{2}x_o'}{\sqrt{\overline{A^2}}\tilde{\omega}}\right) \tag{58}$$

where $F(\cdot)$ is defined by (23) through (25). Averaging (58) over the pdf of $\tilde{\omega}$, (57), and replacing $\overline{A^2}$ by $2\sigma^2$ and x_o' by $S\sqrt{b_1}$, we obtain

$$\tilde{N}(S) = \int_0^\infty X(f) F\left(\frac{\sqrt{b_1}S}{2\pi f\sigma}\right) df. \tag{59}$$

The derivatives of this function with respect to S can be found quite simply, although some caution is required when evaluating them at $S = 0$. The resulting value for $C_2 (= \frac{1}{2}\tilde{N}''(0))$ is found to be

$$C_2 = \lim_{S \to 0} \left\{ \frac{\sqrt{b_1}}{S\sigma^3} \int_0^\infty \frac{[X(f) - X(0)]}{2\pi f} \frac{d}{dS} F\left(\frac{\sqrt{b_1}S}{2\pi f\sigma}\right) df \right\}. \tag{60}$$

For most realistic processes, the continuous part of the power spectrum has zero slope at $f = 0$, i.e., $X'(0) = 0$. In that circumstance, (60) reduces to the much simpler form

$$C_2 = \left(\frac{\pi^2}{12} - 2\right) \frac{b_1}{\sigma^4} \int_0^\infty \frac{[X(f) - X(0)]}{(2\pi f)^2} df; \qquad X'(0) = 0. \tag{61}$$

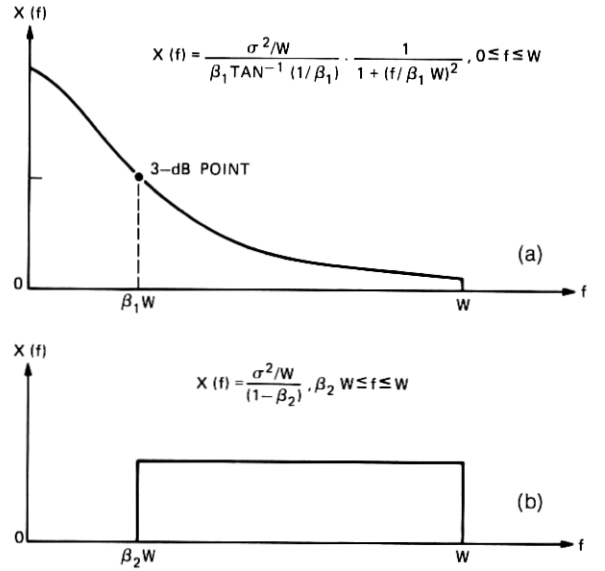

Fig. 12—Two families of spectra. (a) Truncated Butterworth spectrum. (b) Bandpass uniform spectrum.

In general, the above C_2 for the non-Gaussian process $\{\tilde{x}(t)\}$ cannot be compared with the C_2 for the Gaussian process $\{x(t)\}$ since we do not have a result for the latter case that is good for all $X(f)$. We do, however, have exact results under some special conditions on $X(f)$ for which C_2 is expected to be maximally dissimilar for the two processes. The very close agreement observed under these conditions persuades us that (60) is a reliable representation of C_2 for Gaussian processes having *any* $X(f)$.

5.4 *Final Result for* $N_s(S)$

Our final approximation to $N(S \approx 0)$ is (44) with $C_0 = 1$ and C_1 and C_2 given by (55) and (60). Note that when $X(0) = 0$, C_1 is zero and C_2 is negative, so that $N_s(S)$ is convex at the origin; and that when $X(0) \neq 0$, C_1 is negative and C_2 can be either positive or negative, depending on $X(f)$. For a spectrum like the one in Fig. 12b, this implies a functional discontinuity at $\beta_2 = 0$, which can be explained as follows: So long as $\beta_2 \neq 0$, the curvature of $N_s(S)$ is convex at the origin, but it becomes concave at some $S > 0$. As β_2 decreases, the curvature at the origin becomes sharper and the point of inflection occurs at successively lower values of S. Finally, in the limiting case

$\beta_2 = 0$, the point of inflection occurs at $S = 0$ and so $N_s(S)$ becomes concave at the origin. Thus, an abrupt increase in X at f close to 0, reflected in a large negative value of C_2, signifies a very small range of validity and calls for caution in using the new result for $N(S \approx 0)$.

For concreteness, suppose that the continuous part of $X(f)$ increases to a large peak density at some low frequency f_o, where $f_o \ll \sqrt{b_1}/2\pi\sigma$. To obtain a more useful approximation to $N(S \approx 0)$ under such circumstances, C_1 and C_2 should be recomputed as if the point of high density were at $f = 0$ instead of $f = f_o$, i.e., as if the spectrum were $X(f + f_o)$. The resulting $N_s(S)$, (44), then corresponds to a spectrum quite similar to $X(f)$ but without the abrupt change at low f. Consequently, it exhibits the correct "large-scale" curvature at low S while omitting the sharp "small-scale" curvature at S near 0 associated with the true C_1 and C_2. An empirically derived rule-of-thumb that leads to good results in all cases is the following: If $C_2 < -10$, shift the continuous part of $X(f)$ to the left until the nearest high-density peak is at $f = 0$, and recompute C_1 and C_2 for this modified spectrum. Then compute the quantity $C = (0.5\ C_2 - 10\ C_1)$ using these values. If C exceeds the original value of C_2, use the newly computed values of C_1 and C_2; otherwise use the original ones.

VI. GENERAL NOISE POWER FORMULA

We now seek an expression for slope overload noise power $[N_o(S)]$ which is accurate over all S for all spectra and is simple to use. Our approach is to derive separate functional descriptions for the regions $0 < S < 4.0$ and $S \geqq 4.0$. The descriptions are such that the resulting $N_o(S)$ and its first derivative are continuous at the boundary $S = 4.0$.

6.1 $N_o(S)$ *for* $S \geqq 4.0$

The result $N_l(S)$, (43), gives a very accurate approximation to $N(S)$ in the region $S \geqq 3.5$. However, our result for $N_{lb}(S)$, (22) through (25), is quite complicated, and the results for $A(S)$, $B(S)$, and $C(S)$ are available in graphical form only (Fig. 9). We now use these results to derive a simple but still accurate representation for this region.

Taking a suggestion from Rice's analysis,[2] we speculate that $N(S)$ for $S \geqq 4.0$ can be accurately approximated by

$$N(S \geqq 4.0) \doteq \frac{243}{4\sqrt{2\pi}} \frac{b_1^2}{b_2} \frac{\exp(-S^2/2)}{S^5} \cdot [\exp(-\alpha_1 \exp(-\alpha_2 S))] \triangleq N_o(S \geqq 4.0). \quad (62)$$

The quantity preceding the brackets is Rice's result $N_R(S)$, (9), while the bracketed term (with $\alpha_2 > 0$) is a monotonically decreasing function that converges to unity as $S \to \infty$. We choose α_1 and α_2 so that

$$N_o(4.0) = N_l(4.0) \text{ and } N_o'(4.0) = N_l'(4.0).$$

By using the data in Fig. 9 to obtain $A(S)$, $B(S)$, $C(S)$, and their first derivatives at $S = 4.0$, and the data in Fig. 6 to obtain $N_{lb}(S)$ and its first derivative at $S = 4.0$, we obtain

$$\alpha_2 = \frac{0.2141 - 0.024M_3 - 0.196M_4 - 0.067M_5}{0.6394 - 0.057M_3 - 0.426M_4 - 0.093M_5} \tag{63}$$

and

$$\alpha_1 = (0.6394 - 0.057M_3 - 0.426M_4 - 0.093M_5) \exp(4\alpha_2) \tag{64}$$

where M_3, M_4, M_5 are the moment excesses defined by (41). Note that when $X(f)$ is the two-band spectrum, ($M_n = 0$, $n \geqq 3$), α_1 and α_2 reduce to 2.45 and 0.336, respectively.

The above approximation to $N(S \geqq 4.0)$ can be tested by comparing it with the more precise results computed for various spectra using (35) and (37). The indications from such comparisons are that the approximation is accurate to within ± 0.3 dB over $S \geqq 4.0$ for all spectra.

6.2 $N_o(S)$ *for* $0 < S < 4.0$

The analyses of Sections IV and V inform us about $N(S)$ at the extremities of the region $0 < S < 4.0$, but not about the variation in between. To estimate this variation reliably, it is convenient to express $N(S)$ in the form

$$N(S) \equiv G(S)N_{lb}(S) \tag{65}$$

and then seek an approximation to $G(S)$. The latter is a spectrum-dependent function that differs from unity because–and to the extent that–$X(f)$ differs from a two-band spectrum having the moments b_0, b_1, and b_2 (Fig. 3). From physical reasoning given earlier, we expect that $G(S) \to 1$ as $S \to \infty$ and that, as S decreases from high values towards 0, $G(S)$ increases because–and to the extent that–b_3, b_4, etc., exceed the minimum values, (6), corresponding to the two-band spectrum. The maximum value of $G(S)$ should then be its value as $S \to 0$, which is $\sigma^2(b_2/b_1^2)$.

This reasoning is supported by careful scrutiny of the results for $N_l(S)$ and $N_s(S)$, Sections IV and V. From Section IV we can show

that $G(S)$ is a nonincreasing function* for $S \geqq 3.5$ and that it goes to unity as $S \to \infty$. From the results of Section V we can show that $G(S)$ is a nonincreasing function* at $S \approx 0$ and that it goes to $\sigma^2(b_2/b_1^2)$ as $S \to 0$. A logical consequence of these observations is that, for $0 < S < 3.5$, $G(S)$ is either a nonincreasing function, or has at least two extrema. The latter possibility has no physical basis in fact, and so we conclude that $G(S)$ is a nonincreasing function over all S, approaching a maximum value of $\sigma^2(b_2/b_1^2)$ as $S \to 0$ and a minimum value of 1 as $S \to \infty$.

Computations show that the decrease in $G(S)$ over $0 < S < 4.0$ is less than 10 dB for all spectra of possible practical interest. Thus if we can find a functional approximation to the quantity

$$g(S) \triangleq \ln G(S) = \ln \left[\frac{N(S)}{N_{tb}(S)}\right]; \qquad 0 < S < 4.0 \tag{66}$$

that is accurate to within ± 10 percent, the resulting approximation to $G(S)$ will be accurate to within ± 1 dB for all spectra of interest. This accuracy should be possible to achieve since $g(S)$ near $S = 0$ and $S = 4.0$ are known from the results of Sections III, IV, and V, and the above argument persuades us that $g(S)$ is nonincreasing over the region in between.

The function that we use to approximate $g(S)$ is

$$g_o(S) = \ln (\sigma^2 b_2/b_1^2) + a_1 S + a_2[\exp (a_3 S + a_4 S^2) - 1] \tag{67}$$

where $a_1, \cdots a_4$ are chosen to give $g_o'(0)$, $g_o''(0)$, $g_o(4)$, and $g_o'(4)$ the values predicted by the results of Sections III, IV, and V. These values are found by using (66), with $N_s(S)$ and $N_l(S)$ replacing $N(S)$ at $S = 0$ and $S = 4$, respectively. Thus, the following equations must be satisfied:

$$a_1 + a_2 a_3 = C_1; \tag{68}$$

$$a_2(a_3^2 + 2a_4) = 2C_2 - C_1^2 + \left(4 - \frac{\pi^2}{6}\right); \tag{69}$$

$$\ln (\sigma^2 b_2/b_1^2) + 4a_1 + a_2[\exp (4a_3 + 16a_4) - 1] = 0.057M_3 + 0.426M_4 + 0.093M_5; \tag{70}$$

and

$$a_1 + a_2(a_3 + 8a_4) \exp(4a_3 + 16a_4) = -0.024M_3 - 0.196M_4 - 0.067M_5 \tag{71}$$

* In fact, $G(S)$ is a *decreasing* function for all but the two-band spectrum, for which case it is precisely 1.

TABLE I—FORMULA COEFFICIENTS FOR THE BUTTERWORTH SPECTRUM

β_1	a_1	a_2	a_3	a_4
0.02	−0.177	2.26	−3.93	−8.76
0.068	−0.151	1.29	−3.70	−7.04
0.10	−0.137	1.06	−3.75	−6.99
0.25	−0.096	0.66	−3.90	−7.03
0.50	−0.066	0.50	−3.91	−6.67
1.0	−0.047	0.42	−3.86	−6.22
2.0	−0.040	0.38	−3.84	−6.00
∞	−0.036	0.37	−3.83	−5.90

where C_1, C_2 and $M_n (n \geqq 3)$ are given by (55), (60), and (41), respectively.

A set of solutions that is quite accurate in most cases is the following:

$$a_1 = -0.024M_3 - 0.196M_4 - 0.067M_5 \tag{72}$$

$$a_2 = \ln (\sigma^2 b_2 / b_1^2) - 0.155M_3 - 1.210M_4 - 0.361M_5 \tag{73}$$

$$a_3 = \begin{cases} (C_1 - a_1)/a_2; & a_2 > 0 \\ 0; & a_2 = 0 \\ |C_1 - a_1|/a_2; & a_2 < 0 \end{cases} \tag{74}$$

$$a_4 = \begin{cases} \frac{1}{2}\left[\frac{2C_2 - C_1^2 + \left(4 - \frac{\pi^2}{6}\right)}{a_2} - a_3^2\right]; & a_2 > 0. \\ 0; & a_2 \leqq 0 \end{cases} \tag{75}$$

The results for a_3 and a_4 when $a_2 \leqq 0$ are approximations only, but a_2 is nonpositive only when $X(f)$ is relatively narrowband, i.e., when $\sigma^2 b_2 / b_1^2 \approx 1$, in which case $G(S)$ is close to 1 over all S. Hence, these approximations lead to a quite accurate representation of $g(S)$. In the

TABLE II—FORMULA COEFFICIENTS FOR THE UNIFORM SPECTRUM

β_2	a_1	a_2	a_3	a_4
0	−0.036	0.37	−3.83	−5.90
0.05	−0.036	0.32	−4.44	−8.21
0.10	−0.036	0.27	0.14	−11.96
0.20	−0.035	0.17	0.21	−7.58
0.30	−0.033	0.08	0.41	−7.95
0.40	−0.029	0.02	1.44	−18.30
0.50	−0.024	−0.01	−1.76	0
0.80	−0.004	−0.01	−0.43	0
1.0	0	0	0	0

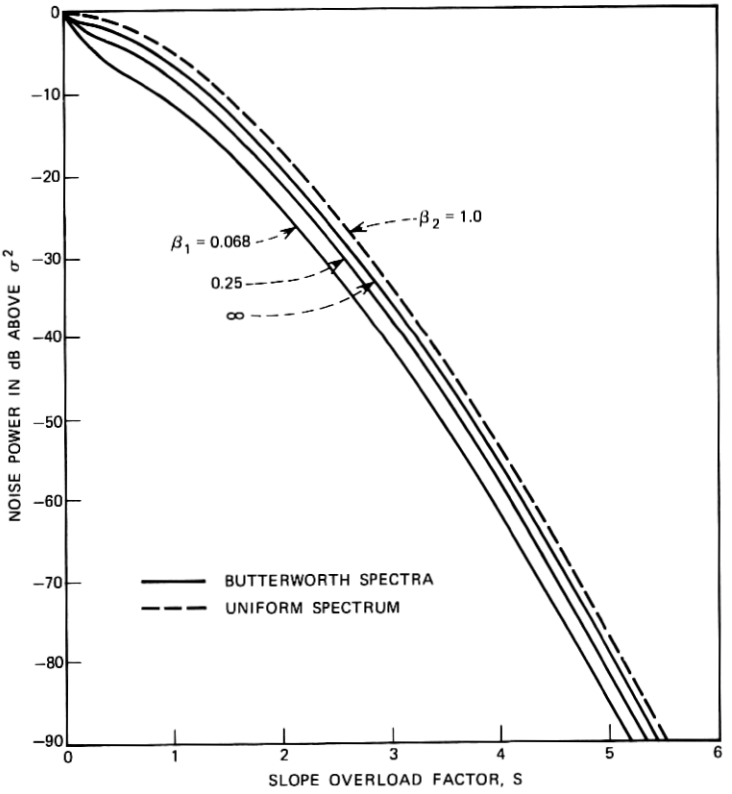

Fig. 13—Noise power results for several spectra.

more usual case where $a_2 > 0$, the above solutions are highly accurate so long as $4a_3 + 16a_4 \leqq -(4 + \ln a_2)$, a condition satisfied for most spectra. If this inequality is violated, solutions for $a_1, \cdots a_4$ can be found by graphical or computerized methods, but such situations appear to be rare.

With $g(S)$ approximated as above, $N_o(S)$ over $0 < S < 4.0$ can be expressed as the product $\exp(g_o(S))N_{tb}(S)$. To obtain a usable expression, however, $N_{tb}(S)$ should be given in a more simple form than eqs. (22) through (25). An approximation to $N_{tb}(S)$ which is accurate to within ± 0.3 dB is

$$N_{tb}(S) \doteq \frac{b_1^2}{b_2}[1 + 2.753S + 2.952S^2] \cdot \exp(-2.753S - 0.341S^2); \qquad 0 < S < 4.0. \quad (76)$$

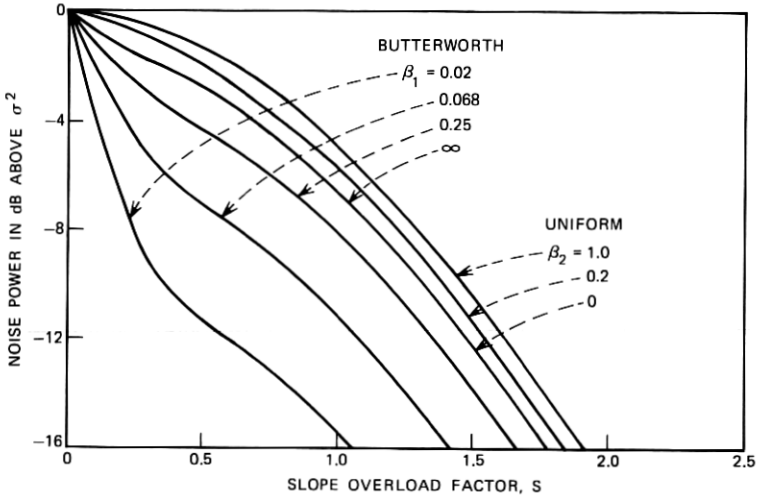

Fig. 14—Noise power results in greater detail.

Combining (76) with (67) leads to the following:

$$N_o(S) = \sigma^2[1 + 2.753S + 2.952S^2] \exp(-0.341S^2) \cdot \exp\{(a_1 - 2.753)S + a_2[\exp(a_3S + a_4S^2) - 1]\}; \quad 0 < S < 4.0. \quad (77)$$

6.3 *Final Expression*

A highly accurate two-region approximation to $N(S)$ is given by the combination of (62) and (77). We have determined, however, that (77) alone predicts $N(S)$ with an accuracy of 1 dB or better for S between 4.0 and 6.5 for all spectra. Moreover, we have determined that $N(S)$ is at least 119 dB below σ^2 for $S \geqq 6.5$ and for all spectra. Obviously, then, (77) can be used over all S for which $N(S)$ is not negligibly small. We therefore present (77) as our final expression for slope overload noise power, with $a_1, \cdots a_4$ defined by (68) through (71) and accurately approximated by (72) through (75) in virtually all cases.

VII. NUMERICAL RESULTS

The new result has been applied to the two families of spectra shown in Fig. 12. The Butterworth spectrum is characterized by an upper truncation frequency (W) and the ratio (β_1) of the 3-dB corner frequency to W. Note that, when $\beta_1 \rightarrow \infty$, the spectrum approaches that

TABLE III—N_P/N_o IN dB FOR THE BUTTERWORTH SPECTRUM

S \ γ	0.036 ($\beta_1 = 0.02$)	0.111 ($\beta_1 = 0.068$)	0.289 ($\beta_1 = 0.25$)	0.556 ($\beta_1 = \infty$)
1.0	+2.85	+1.76	+1.44	+1.70
2.0	+0.41	−0.20	−0.22	−0.10
3.0	+0.43	−0.01	−0.04	+0.22
4.0	+0.96	+0.74	+0.71	+0.81
5.0	+1.14	+1.12	+1.11	+1.13
6.0	+0.90	+0.85	+0.80	+0.70

of bandlimited white noise. The bandpass uniform spectrum is characterized by an upper truncation frequency (W) and the ratio (β_2) of the lower truncation frequency to W. Note that $\beta_2 = 0$ corresponds to bandlimited white noise in this case and that, as $\beta_2 \to 1$, the spectrum becomes infinitely narrowband.

For each of these two families, the formula coefficients, (a_1, a_2, a_3, a_4), have been computed as functions of the respective β-parameter. The results for the Butterworth spectrum are given by Table I and those for the uniform spectrum by Table II. The values shown are rounded to the decimal accuracy required.

Curves of N_o/σ^2 versus S for several Butterworth spectra of practical interest and for the narrowband spectrum are shown in Fig. 13. (The curve for the narrowband case represents an upper bound on $N(S)/\sigma^2$ for all spectra.) Also, an informative closeup that treats more spectra but over a reduced range of S is given by Fig. 14.

Since the new formula is highly accurate for all spectra, it can be used to estimate the accuracy of the Protonotarios formula, (10). Table III compares $N_P(S)$ with $N_o(S)$ for various Butterworth spectra spanning the range of $\gamma = b_1^2/b_2 b_0$ of practical interest, while Table IV gives the comparison for various two-band spectra. The larger errors in Table IV must be regarded as untypical, since the two-band spectrum itself is rather artificial. For more typical spectra, we can

TABLE IV—N_P/N_o IN dB FOR THE TWO-BAND SPECTRUM

S \ γ	0.111	0.289	0.556	1
1.0	+5.04	+3.55	+2.49	+1.52
2.0	+2.45	+1.46	+0.75	+0.06
3.0	+1.97	+1.23	+0.70	+0.19
4.0	+2.05	+1.54	+1.12	+0.71
5.0	+1.79	+1.55	+1.30	+1.02
6.0	+0.84	+0.88	+0.74	+0.50

expect the errors in the Protonotarios formula for given S and γ to be more like the entries in Table III.

VIII. CONCLUSION

Aside from providing a new formula for slope overload noise power, this work has served to resolve the disparities between previously published formulas and can be used to identify the accuracies and limitations of those most widely used. Furthermore, the new result and the underlying methods of analysis can be extended to treat other important topics that have been mostly ignored before. Among these are the average duty cycle of slope overload, the slope overload noise spectrum, the effects of leaky feedback integrators on slope overload noise power, and the slope overload noise power for certain non-Gaussian processes.

IX. ACKNOWLEDGMENTS

The author is indebted to D. J. Goodman for his suggestions and encouragement throughout the execution of this work, and to D. L. Duttweiler for a number of helpful comments.

REFERENCES

1. Zetterberg, L. H., "A Comparison Between Delta and Pulse Code Modulation," Ericsson Technics, *2*, No. 1 (January 1955), pp. 95–154.
2. O'Neal, J. B., Jr., "Delta Modulation Quantizing Noise Analytical and Computer Simulation Results for Gaussian and Television Input Signals," B.S.T.J., *45*, No. 1 (January 1966), pp. 117–141.
3. Protonotarios, E. N., "Slope Overload Noise in Differential Pulse Code Modulation Systems," B.S.T.J., *46*, No. 9 (November 1967), pp. 2119–2162.
4. Abate, J. E., "Linear and Adaptive Delta Modulation," Proc. IEEE, *55* (March 1967), pp. 298–308.
5. van de Weg, H., "Quantizing Noise of a Single Integration Delta Modulation System With an N-Digit Code," Phillips Res. Rpt., *8* (1953), pp. 367–385.
6. Goodman, D. J., "Delta Modulation Granular Quantizing Noise," B.S.T.J., *48*, No. 5 (May-June 1969), pp. 1197–1218.
7. Iwersen, J. E., "Calculated Quantizing Noise of Single-Integration Delta-Modulation Coders," B.S.T.J., *48*, No. 7 (September 1969), pp. 2359–2389.
8. Rice, S. O., "Mathematical Analysis of Random Noise," B.S.T.J., *23*, No. 3 (July 1944), pp. 282–332, and *24*, No. 1 (January 1945), pp. 46–156.
9. Aaron, M. R., Fleischman, J. S., McDonald, R. A., and Protonotarios, E. N., "Response of Delta Modulation to Gaussian Signals," B.S.T.J., *48*, No. 5 (May-June 1969), pp. 1167–1195.
10. Greenstein, L. J., unpublished work.